

Binary relaxor piezoceramic Pb (Mg_{1/3}Nb_{2/3}) O₃-PbTiO₃ for energy harvesting

Bomkesh Bhoi, Pranati Purohit

School of Physics, Gangadhar Meher University, Sambalpur, India

Article Info

Article history:

Received Mar 26, 2024

Revised Nov 22, 2024

Accepted Jan 26, 2025

Keywords:

Energy harvesting

Lead magnesium niobate Pb

(Mg_{1/3}Nb_{2/3}) O₃-lead titanate

PbTiO₃ (PMN-PT)

Perovskite structure

Piezoelectric materials

Relaxor-PT

ABSTRACT

Perovskite relaxor-PT piezoelectrics are suitable materials for energy harvesting. Relaxor-PT crystals have electromechanical properties that can replace lead zirconate titanate (PZT). However, the growth of these relaxor-PT crystals is tedious and expensive. The important parameter for energy harvesting is the transduction rate ($d \times g$) where d represents the piezoelectric coefficient and g represents the piezoelectric voltage constant. There is always a challenge to obtain a high ($d \times g$) value. Lead magnesium niobate Pb (Mg_{1/3}Nb_{2/3}) O₃-lead titanate PbTiO₃ (PMN-PT) is a binary relaxor-PT ceramic and the morphotropic phase boundary (MPB) of (1- x) PMN- x PT ceramics occur around $x=0.29-0.40$ which is not exactly defined. So here we have synthesized 0.71PMN-0.29PT, 0.68PMN-0.32PT, and 0.65PMN-0.35PT compositions by two-step sintering solid-state method. The x-ray diffraction (XRD) patterns of the PMN-PT ceramics exhibit a characteristic perovskite structure and also show that PMN-PT ceramics fall within the region of MPB. Out of the three compositions, the 0.71PMN-0.29PT ceramics show a higher transduction rate ($d \times g$). So, this piezoelectric ceramic has the potential to replace costly piezoelectric single crystals in the creation of affordable, high-frequency energy harvesting devices.

This is an open access article under the [CC BY-SA](https://creativecommons.org/licenses/by-sa/4.0/) license.



Corresponding Author:

Pranati Purohit

School of Physics, Gangadhar Meher University

Amruta Vihar, Sambalpur Odisha, Pin-768004, India

Email: pranatipurohit@gmail.com

1. INTRODUCTION

Lead magnesium niobate Pb (Mg_{1/3}Nb_{2/3}) O₃ (PMN) is a relaxor ferroelectric material, which can be studied further concurrently with theoretical as well as practical applications [1]–[3]. Adding PbTiO₃ (PT) to PMN enhances the dielectric characteristics of the material. The PMN-PT (Pb (Mg_{1/3}Nb_{2/3}) O₃+PbTiO₃) solid composition emerges between PMN and PbTiO₃ creating a morphotropic phase boundary (MPB) within the compositional range of 0.27 to 0.34 for x , where rhombohedral and tetragonal phases coexist [4]. Single crystals of PMN-PT with compositions near MPB have been documented to demonstrate remarkably elevated piezoelectric coefficients (d), exceedingly substantial piezoelectric strain (S), and exceptionally elevated electromechanical coupling factors (k) [5]–[7]. However, the growth of these relaxor-PT single crystals is tedious and expensive. To overcome this problem research shifts towards piezoceramic materials, as it is cost-effective and easy to fabricate with different shapes and sizes.

The energy density of piezoceramic material is the product of piezoelectric coefficients (d) and piezoelectric voltage constant (g) [8], [9]. The available vibrational energy can be converted into electrical energy by different transduction mechanisms, out of which the piezoelectric energy harvesting mechanism can be used to harvest energy from a micro-to-meso scale. In piezoelectric energy harvesting, the output

power of the energy harvester will depend on the frequency of the materials used. The output power will be maximum for low resonant frequency materials, but the identification of a low resonant frequency material is difficult. Kim *et al.* [10] considered the transduction rate ($d \times g$) of the material in place of resonant frequency. The output will be maximum for the material with higher transduction rate. In this study, we present a straightforward approach for creating micrometre-sized, pure perovskite (1-x) PMN-xPT powder where $x=0.29, 0.32,$ and 0.35 by two step sintering solid state method. X-ray diffraction (XRD) analysis provide a clear confirmation of a stable morphotropic phase that is situated in between rhombohedral and tetragonal phases. Here we have examined the energy harvesting utilizing a '33' mode, where mechanical stress and/or electric field are along the direction of polarization. The transduction rate ($d_{33} \times g_{33}$) of these materials were measured and analysed for energy harvesting applications.

2. RESEARCH METHOD

PMN-PT powders were synthesized with a specified composition of (1-x) Pb ($Mg_{1/3}Nb_{2/3}$) O_3 -xPbTiO₃ by a two-step sintering solid-state reaction technique as shown in Figure 1. High-purity powder of the following oxides, Pb₃O₄, MgO, TiO₂, and Nb₂O₅, each exceeding 99.0% purity was taken as the starting materials and the B-site precursor method was implemented to prevent the development of a pyrochlore second phase. This approach involved pre-reacting the necessary MgO with Nb₂O₅ to produce the columbite phase [11]. The columbite powders obtained from this phase were combined with the remaining powder oxides by using a mortar and pestle for 8 hours and adding methanol during the mixing. The mixture underwent calcination at 950 °C for 4 hours, then it was ground for an additional 8 hours by mortar and pestle, which yields PMN-PT powders in a pure perovskite state.

After adding a binder comprising 5% by weight of polyvinyl alcohol, the PMN-PT powder was pressed uniaxially by using a hydraulic press into disks of diameter 13 mm with a pressure of about 100-120 Mpa. The compressed samples were subjected to firing at 600 °C for a duration of 2 hours to eliminate the binder. Subsequently, the specimens underwent sintering at 1,250 °C for 2 hours. To prevent the evaporation of Pb from this, the pellets were encased using protective powders of identical composition, enclosed within a sealed crucible throughout the sintering procedure. Then the product obtained was smoothed down to a thickness of 2 mm by using sandpaper.

After sintering, the samples with apparent densities were measured using geometrical methods. The samples' crystal structures were analyzed using an x-ray diffractometer, employing Cu-K α radiation. The scanning process covered a 2 θ range from 20 to 80, with a step size of 0.020. Fourier transform infrared spectroscopy (FTIR) was done in the wavenumber range of 400-5,000 cm⁻¹ to monitor the phase change of functional groups. For electrical characterization, the silver coating was applied on both sides of the polished ceramic pellets and heated at 600 °C for 20 minutes to ensure proper electrical contact. The samples were then subjected to polarization by applying a direct current (DC) field of 20 kV/cm submerged in a silicon oil bath for a duration of 2-4 hours using a specific polling setup consisting of a DC-power supply and a voltage amplifier with a multimeter for voltage reading. Following a 24-hour polling period, the piezoelectric coefficient d_{33} was assessed using a piezoelectric d_{33} -meter (Sinocera, Model YE2730A). The LCR meter (SM5118) was used for the study of dielectric properties. At 25 °C, the capacitance (C), impedance, and dissipation factor (tan δ) were determined. This analysis was performed for all the compositions of PMN-PT ceramic pellets. The dielectric constant was subsequently calculated using the parallel-plate capacitor equation, represented as $\epsilon_r = \frac{Ct}{\epsilon_0 A}$. In this equation, C stands for specimen capacitance, t, and A respectively denote the thickness and surface area of the specimens, and ϵ_0 represents the dielectric permittivity in free space.

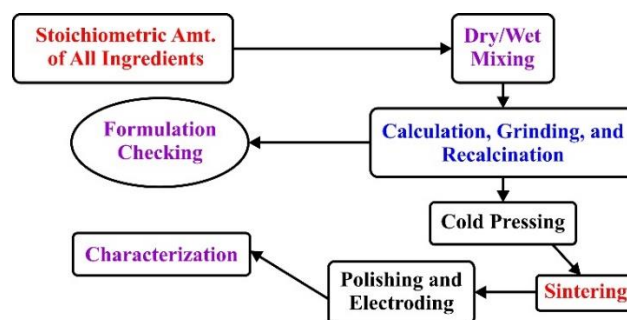


Figure 1. Synthesis of PMN-PT by solid-state reaction method

3. RESULTS AND DISCUSSION

3.1. FTIR analysis

FTIR spectroscopy can be used to monitor changes in ceramic powder as it undergoes thermal reactions to produce perovskite oxide powders. Figure 2 illustrates the infrared (IR) spectra obtained using FTIR of the PMN-PT powders for various compositions in the 400-5,000 cm^{-1} range. This spectrum displayed a wide band spanning from 850 to 570 cm^{-1} , with the highest absorbance observed around 609 cm^{-1} . This particular peak was assigned to the vibration of B-O (where B=Mg, Nb, and Ti) bonds within the systems.

The IR spectrum of PMN-PT shares similarities with most other ABO_3 -type perovskite compounds, showing four distinct vibration modes [12], [13]. Figure 2 displays two absorption bands. The first one is an asymmetric band, ν_1 -stretching, with a higher frequency ranging from 850 to 570 cm^{-1} and centered around 572 cm^{-1} . This band represents the combined normal vibration modes of ν_1 - NbO_3 , ν_1 - TiO_3 , and ν_1 - MgO_3 stretching along the spontaneous polarization in the PMN-PT structure. The ν_1 band is associated with the BO_6 octahedron bond and indicates perovskite phase formation at all compositions of $(1-x)$ PMN- x PT, with the proportion increasing as the rises in PT contains.

The mid-IR spectra do not exhibit bands related to Pb ions due to their heavy masses. The second band, ν_2 -bending, occurs at a lower frequency beyond the experimental range, starting from 400 cm^{-1} , and is assigned to B-O bending normal vibration. However, in this study, the other two bands, ν_3 -cation- (BO_3) lattice mode, and ν_4 -bending vibrations, fall under the available experimental frequency range (400–4,000 cm^{-1}).

3.2. X-Ray diffraction analysis

The solid-state reaction process for PMN or PMN-based phases is widely recognized as highly intricate. In this procedure, the perovskite phase formation of PMN does not take place directly from the oxides [14]. Instead, the reaction begins with PbO and Nb_2O_5 at approximately 600 $^\circ\text{C}$, forming a cubic pyrochlore compound ($\text{Pb}_2\text{Nb}_2\text{O}_7$). This cubic pyrochlore ($\text{Pb}_2\text{Nb}_2\text{O}_7$) further reacts with MgO, leading to the form of perovskite PMN which also includes the existence of $\text{Pb}_2\text{Nb}_2\text{O}_7$ at a higher temperature of 800 $^\circ\text{C}$. By adding excess amounts of PbO and MgO, the $\text{Pb}_2\text{Nb}_2\text{O}_7$ phase was minimized, and obtaining a single-phase PMN through the solid-state process remains highly challenging. In our study, Figure 3 displays the XRD results for fully sintered PMN-PT ceramics, with the highest perovskite content and bulk density. These patterns illustrate the presence of fully developed perovskite structures across all compositions. In the spectrum there is no significant peak splitting was observed which indicates that these PMN-PT ceramic composition falls within the range of MPB, where both rhombohedral as well as tetragonal phases coexist.

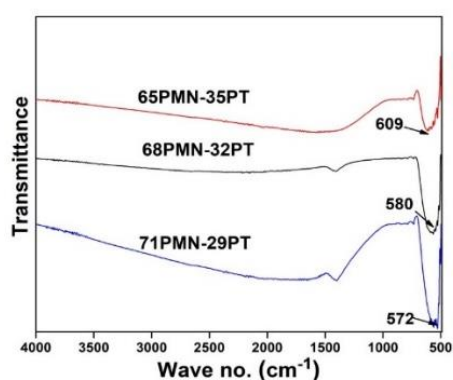


Figure 2. FTIR spectra of $(1-x)$ PMN- x PT powders, where $x=0.29, 0.32, \text{ and } 0.35$

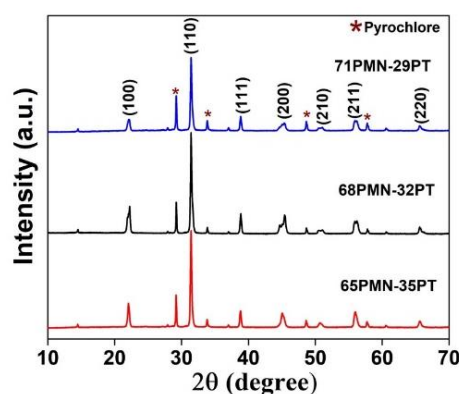


Figure 3. XRD patterns of $(1-x)$ PMN- x PT ceramic

3.3. Density

The densities of $(1-x)$ PMN- x PT ceramics as they undergo the process of sintering are given in Table 1. These densities were determined using geometric calculations. From Table 1, it was observed that with the increase in the value of x , there was a slight reduction in the bulk density. This phenomenon was ascribed to the comparatively lower melting point of PT. In this study all the pellets possess the highest relative density as all underwent sintering with a temperature of about 1,220-1,250 $^\circ\text{C}$ with a grain size of the order of micrometer which is the same as the previously reported PMN-PT sintering values [15].

3.4. Dielectric properties

The dielectric constant (ϵ_r) of all the pooled and unpooled samples was measured at room temperature with the application of one kHz frequency and tabulated in Table 1. Before or after poling in both cases 0.71PMN-0.29PT has the highest dielectric constant. It is found that there is a fall in the value of ϵ_r by adding more PT to PMN. The sample that lies at the morphotropic phase boundary always shows a higher dielectric constant and piezoelectric constant. This confirms that 0.71PMN-0.29PT is the MPB composition. The loss factor ($\tan\delta$) is also less than 0.05. As we work with ceramics containing unsymmetrically oriented grains and partially existing symmetries, several factors are taken into consideration. These factors are the role of lattice extension and rotation while doing polarization, as well as the reversible domain-wall reaction to low-field excitation [16], [17]. The impact of other interfaces such as polar nanoregions, or interphase boundaries [18]–[20], all of which collectively contribute to the measured permittivity. The potential impact of grain boundaries between the various compositions is not taken into account in this analysis, considering that the grain size in our ceramics remains relatively uniform across all compositions. In unpoled PMN-PT ceramics, the 29PT composition exhibits the highest dielectric permittivity (ϵ_r) among others. This composition features an R/M phase symmetry and shows minimal ferroelectric lattice distortion. At room temperature using the DC polarisation method, the permittivity decreases in all compositions. It is essential to address two key factors regarding the composition-dependent changes in permittivity after poling. The first factor involves the extrinsic contribution to permittivity arising from domain walls or similar interfaces, including their movement and density [21]–[23]. This can lead to a reduction in permittivity when there's a reduction in the number of domain walls after polarization as the growth of domains aligned in a favorable direction [24]. The second factor is the variation in permittivity due to anisotropy, which is influenced by the lattice symmetry and its alignment with respect to the direction of the applied field [25], [26]. In PMN-PT, both the R/M and T phases on either side of the MPB exhibit a significant dielectric anisotropy, where the transverse permittivity (ϵ_{11}) is more than the longitudinal permittivity (ϵ_{33}). This property was earlier mentioned which is also known as "rotator ferroelectrics" [27]. This anisotropy is increased at the MPB between R/M and T phase. During poling the spontaneous polarization reverses along the applied field direction. This is anticipated that in poled samples there will be an increase in the contribution from ϵ_{33} , which will be balanced by a reduction in the contribution from ϵ_{11} . Consequently, this should result in decrease in the overall permittivity after poling.

Table 1. Dielectric properties of (1-x) PMN-xPT before and after poling

Composition	Density (10^3 kg/m ³)	Before Poling			After Poling		
		Capacitance (C)	Dissipation factor ($\tan\delta$)	Dielectric constant (ϵ_r)	Capacitance (C)	Dissipation factor ($\tan\delta$)	Dielectric constant (ϵ_r)
0.71PMN-0.29PT	6.46	1.220 nF	0.029	2390	896 pF	0.025	1755
0.68PMN-0.32PT	6.23	1.048 nF	0.025	2071	635 pF	0.022	1255
0.65PMN-0.35PT	6.04	851 pF	0.028	1740	490 pF	0.015	1002

3.5. Piezoelectric coefficient

After subjecting the ceramic pallet to a DC poling of 2 to 4 hours, the direct piezoelectric coefficient, d_{33} of the PMN-PT ceramics was measured and given in Table 2. The peak d_{33} value occurs at the 0.71PMN-0.29PT composition, which signifies the MPB between the monoclinic (M) Pm symmetry and the tetragonal (T) P4mm. As the ceramics consist of grains with crystallographic orientations that are randomly oriented, hence their response to the external electric field is enhanced by the collective response of lattice strain and interface movements, encompassing the motion of the domain walls and interphase boundaries. It can be reasonably argued that the simultaneous symmetries present at the MPB play a role in creating a flattened free energy landscape and lower energy barriers [28]. This, in turn, facilitates the occurrence of the most significant lattice distortion which leads to maximum polarization and strain response.

Table 2. Piezoelectric properties of (1-x) PMN-xPT for x=29, 32, and 35

Composition	d_{33} pC/N	g_{33} (10^{-3} Vm/N)	$d_{33} \times g_{33}$ (10^{-15} m ² /N)
0.71PMN-0.29PT	114	7.34	836.76
0.68PMN-0.32PT	90	8.10	729
0.65PMN-0.35PT	58	6.54	379.32

3.6. Piezoenergy harvesting

In the context of energy harvesting, the generated power of a piezoenergy harvester is dependent upon the resonant frequency of the piezoceramic materials. For the output power to be higher the resonance frequency must be low but the synthesis of such materials with low resonance frequency is a tedious task. Therefore, in this method, we choose the off-resonance condition to enhance the output power that is the transduction rate ($d_{33} \times g_{33}$) of the piezoceramic material [10]. The material with high d_{33} and g_{33} product will generate high power. Also, it is difficult to achieve the high $d_{33} \times g_{33}$ value as any increase in piezoelectric constant (d) is associated with an increase in dielectric permittivity (ϵ_r) and a decrease in piezoelectric voltage constant (g) as $g = \frac{d}{\epsilon_0 \epsilon_r}$. The maximum output power was estimated using (1).

$$P = \frac{1}{2} (d_{33} \times g_{33}) \times \left(\frac{F}{A}\right)^2 \times (At) \quad (1)$$

Where ‘F’ is the force applied on the material, ‘A’ and ‘t’ represent the area of the cross-section and the thickness of the pellet respectively. The data reported in Table 2 represents that by increasing the PT contains the value of d_{33} decreases corresponding transduction rate also decreases. At the MPB region, the materials have a high value of dielectric constant and d_{33} , which justifies the previous study done on other materials in off-resonance conditions. This study confirms that the MPB composition for this binary material is 0.71PMN-0.29PT and the ceramic pellets can give maximum output power when used in energy harvester. For energy harvesting the output not only depends on the type of piezoceramic materials but also on the design of the energy harvester and the electric circuit. The equation of power depends on the transduction rate and the thickness, it is better to design a stack-type energy harvester.

4. CONCLUSION

Here we have synthesized 0.71PMN-0.29PT, 0.68PMN-0.32PT, and 0.65PMN-0.35PT compositions by two-step sintering solid-state method. The 0.71PMN-0.29PT composition lies in the MPB region which was confirmed by both XRD and FTIR analysis. Further, the pellets of this composition of pellets show the highest d_{33} value as 114 pC/N, maximum dielectric constant ϵ_r value of 1,755, and exhibited the highest transduction rate ($d_{33} \times g_{33}$) value as $837 \times 10^{-15} \text{ m}^2/\text{N}$. These findings provide a breakthrough in developing power sources capable of satisfying low power demands. This can also be extended through proper investigation by a more detailed study on energy harvesting. This is crucial for refining the modes of energy harvesters and electric circuits for energy harvesting applications which is left for future research.

ACKNOWLEDGEMENTS

This work was supported by the Department of Higher Education Odisha (OURIIP SEED fund-2020/51-Physics).





REFERENCES

- [1] L. E. Cross, “Relaxorferroelectrics: an overview,” *Ferroelectrics*, vol. 151, no. 1, pp. 305–320, Jan. 1994, doi: 10.1080/00150199408244755.
- [2] P. Purohit, Y. K. Yadav, and S. S. K. Titus, “Low force measurement based on impedance of a piezo-resonator,” *MAPAN*, vol. 32, no. 4, pp. 293–296, Dec. 2017, doi: 10.1007/s12647-017-0219-3.
- [3] P. Purohit, Y. K. Yadav, and S. K. Jain, “A study of determination of dynamic viscosity in liquids using radial mode piezo-resonator,” *Ferroelectrics*, vol. 519, no. 1, pp. 236–240, Oct. 2017, doi: 10.1080/00150193.2017.1362273.
- [4] A. K. Singh and D. Pandey, “Evidence for M_B and M_C phases in the morphotropic phase boundary region of $(1-x)$ [Pb ($Mg_{1/3} Nb_{2/3}$) O_3] $-x$ PbTiO₃: a rietveld study,” *Phys. Rev. B*, vol. 67, no. 6, p. 064102, Feb. 2003, doi: 10.1103/PhysRevB.67.064102.
- [5] B. Bhoi and P. Purohit, “A brief review on the status of binary and ternary relaxor-PT materials,” *Mater. Today Proc.*, vol. 62, pp. 5298–5301, 2022, doi: 10.1016/j.matpr.2022.03.366.
- [6] S.-E. Park and T. R. Shrout, “Ultrahigh strain and piezoelectric behavior in relaxor based ferroelectric single crystals,” *J. Appl. Phys.*, vol. 82, no. 4, pp. 1804–1811, Aug. 1997, doi: 10.1063/1.365983.
- [7] B. Bhoi and P. Purohit, “A study on effect of doping on piezoelectric materials,” in *2022 International Interdisciplinary Conference on Mathematics, Engineering and Science (MESIICON)*, IEEE, Nov. 2022, pp. 1–6. doi: 10.1109/MESIICON55227.2022.10093306.
- [8] R. A. Islam and S. Priya, “High-Energy density ceramic composition in the system Pb(Zr,Ti)O₃-Pb[(Zn,Ni)_{1/3} Nb_{2/3}]O₃,” *J. Am. Ceram. Soc.*, vol. 89, no. 10, pp. 3147–3156, Oct. 2006, doi: 10.1111/j.1551-2916.2006.01205.x.
- [9] S. Priya, “Criterion for material selection in design of bulk piezoelectric energy harvesters,” *IEEE Trans. Ultrason. Ferroelectr. Freq. Control*, vol. 57, no. 12, pp. 2610–2612, Dec. 2010, doi: 10.1109/TUFFC.2010.1734.
- [10] H. W. Kim, S. Priya, K. Uchino, and R. E. Newnham, “Piezoelectric energy harvesting under high pre-stressed cyclic vibrations,” *J. Electroceramics*, vol. 15, no. 1, pp. 27–34, Sep. 2005, doi: 10.1007/s10832-005-0897-z.
- [11] A. Badel, A. Benayad, E. Lefevre, L. Lebrun, C. Richard, and D. Guyomar, “Single crystals and nonlinear process for





- outstanding vibration-powered electrical generators,” *IEEE Trans. Ultrason. Ferroelectr. Freq. Control*, vol. 53, no. 4, pp. 673–684, Apr. 2006, doi: 10.1109/TUFFC.2006.1611027.
- [12] S. L. Swartz and T. R. Shrout, “Fabrication of perovskite lead magnesium niobate,” *Mater. Res. Bull.*, vol. 17, no. 10, pp. 1245–1250, Oct. 1982, doi: 10.1016/0025-5408(82)90159-3.
- [13] C. H. Perry, B. N. Khanna, and G. Rupprecht, “Infrared studies of perovskite titanates,” *Phys. Rev.*, vol. 135, no. 2A, pp. A408–A412, Jul. 1964, doi: 10.1103/PhysRev.135.A408.
- [14] T. R. Shrout and A. Halliyal, “Preparation of lead-based ferroelectric relaxors for capacitors,” *Am. Ceram. Soc. Bull.*, vol. 66, no. 4, pp. 704–711, 1987, [Online]. Available: <http://bit.ly/4hRKEsH>
- [15] R. Wongmaneerung, A. Rittidech, O. Khamman, R. Yimnirun, and S. Ananta, “Processing and properties of $\text{Pb}(\text{Mg}_{1/3}\text{Nb}_{2/3})\text{O}_3$ - PbTiO_3 -based ceramics,” *Ceram. Int.*, vol. 35, no. 1, pp. 125–129, Jan. 2009, doi: 10.1016/j.ceramint.2007.10.037.
- [16] P. M. Shepley, L. A. Stoica, Y. Li, G. Burnell, and A. J. Bell, “Effects of poling and crystallinity on the dielectric properties of $\text{Pb}(\text{In}_{1/2}\text{Nb}_{1/2})\text{O}_3$ - $\text{Pb}(\text{Mg}_{1/3}\text{Nb}_{2/3})\text{O}_3$ - PbTiO_3 at cryogenic temperatures,” *Sci. Rep.*, vol. 9, no. 1, p. 2442, Feb. 2019, doi: 10.1038/s41598-019-38995-9.
- [17] J. Peräntie, J. Hagberg, A. Uusimäki, J. Tian, and P. Han, “Characteristics of electric-field-induced polarization rotation in $\langle 001 \rangle$ -poled $\text{Pb}(\text{Mg}_{1/3}\text{Nb}_{2/3})\text{O}_3$ - PbTiO_3 single crystals close to the morphotropic phase boundary,” *J. Appl. Phys.*, vol. 112, no. 3, Aug. 2012, doi: 10.1063/1.4745902.
- [18] M. E. Manley *et al.*, “Giant electromechanical coupling of relaxor ferroelectrics controlled by polar nanoregion vibrations,” *Sci. Adv.*, vol. 2, no. 9, Sep. 2016, doi: 10.1126/sciadv.1501814.
- [19] V. Westphal, W. Kleemann, and M. D. Glinchuk, “Diffuse phase transitions and random-field-induced domain states of the ‘relaxor’ ferroelectric $\text{PbMg}_{1/3}\text{Nb}_{2/3}\text{O}_3$,” *Phys. Rev. Lett.*, vol. 68, no. 6, pp. 847–850, Feb. 1992, doi: 10.1103/PhysRevLett.68.847.
- [20] J. L. Jones *et al.*, “Domain wall and interphase boundary motion in a two-phase morphotropic phase boundary ferroelectric: frequency dispersion and contribution to piezoelectric and dielectric properties,” *Phys. Rev. B*, vol. 86, no. 2, p. 024104, Jul. 2012, doi: 10.1103/PhysRevB.86.024104.
- [21] S. Liu and R. E. Cohen, “Origin of stationary domain wall enhanced ferroelectric susceptibility,” *Phys. Rev. B*, vol. 95, no. 9, p. 094102, Mar. 2017, doi: 10.1103/PhysRevB.95.094102.
- [22] P. Chu *et al.*, “Kinetics of 90° domain wall motions and high frequency mesoscopic dielectric response in strained ferroelectrics: a phase-field simulation,” *Sci. Rep.*, vol. 4, no. 1, p. 5007, May 2014, doi: 10.1038/srep05007.
- [23] J. Liu *et al.*, “Impact of alternating current electric field poling on piezoelectric and dielectric properties of $\text{Pb}(\text{In}_{1/2}\text{Nb}_{1/2})\text{O}_3$ - $\text{Pb}(\text{Mg}_{1/3}\text{Nb}_{2/3})\text{O}_3$ - PbTiO_3 ferroelectric crystals,” *J. Appl. Phys.*, vol. 128, no. 9, Sep. 2020, doi: 10.1063/5.0020109.
- [24] Y. L. Wang, Z. B. He, D. Damjanovic, A. K. Tagantsev, G. C. Deng, and N. Setter, “Unusual dielectric behavior and domain structure in rhombohedral phase of BaTiO_3 single crystals,” *J. Appl. Phys.*, vol. 110, no. 1, Jul. 2011, doi: 10.1063/1.3605494.
- [25] F. Li, S. Zhang, J. Luo, X. Geng, Z. Xu, and T. R. Shrout, “[111]-oriented PIN-PMN-PT crystals with ultrahigh dielectric permittivity and high frequency constant for high-frequency transducer applications,” *J. Appl. Phys.*, vol. 120, no. 7, Aug. 2016, doi: 10.1063/1.4961202.
- [26] M. Davis, D. Damjanovic, and N. Setter, “Correlation between dielectric anisotropy and positive or zero transverse piezoelectric coefficients in perovskite ferroelectric single crystals,” *Appl. Phys. Lett.*, vol. 87, no. 10, Sep. 2005, doi: 10.1063/1.2041827.
- [27] M. Davis, M. Budimir, D. Damjanovic, and N. Setter, “Rotator and extender ferroelectrics: importance of the shear coefficient to the piezoelectric properties of domain-engineered crystals and ceramics,” *J. Appl. Phys.*, vol. 101, no. 5, Mar. 2007, doi: 10.1063/1.2653925.
- [28] A. A. Heitmann and G. A. Rossetti, “Thermodynamics of ferroelectric solid solutions with morphotropic phase boundaries,” *J. Am. Ceram. Soc.*, vol. 97, no. 6, pp. 1661–1685, Jun. 2014, doi: 10.1111/jace.12979.

BIOGRAPHIES OF AUTHORS



Bomkesh Bhoi     received his Ph. D degree from Gangadhar Meher University, Sambalpur, Odisha, India. He completed his M. Sc in physics from G.M. (Autonomous) College, Sambalpur affiliated with Sambalpur University. He has been working as a lecturer in physics at Burla N.A.C. College, Burla since 2016. He has more than 7 years of teaching experience and published research papers in reputed journals. His research interest includes piezoelectric materials and their applications. He can be contacted at email: abhinash373@gmail.com.



Pranati Purohit     is an experienced assistant professor in the School of Physics, Gangadhar Meher University, Sambalpur, Odisha since 2020. Before this, she was working as an Assistant Professor in the Department of Applied Sciences, The NorthCap University, Gurugram, Haryana. She completed her M. Sc in Physics from Utkal University. Dr. Pranati received her MPhil and Ph. D degrees from Sambalpur University. She has twenty years of UG and PG teaching experience. She has published research papers in various high-impact journals of international and national repute. Currently, she is engaged in piezoelectric materials and devices research. She was awarded a project amounting to five lakhs from the Department of Higher Education, Government of Odisha under the OURIP seed fund scheme. She is currently working on a seed fund project of one lakh by Gangadhar Meher University. She can be contacted at email: pranatipurohit@gmail.com.